

# The Effects of Crater Topography on Surface Wind Patterns as Recorded by Dune Fields on Mars

Joe Zhang

August 6, 2017

## Abstract

Deciphering the climatic history of Mars requires an understanding of current climate and weather. One important aspect of Martian weather modelling consists of global wind patterns. Current Global Climate Models (GCMs) of the Martian atmosphere correlate poorly with local wind directions defined over cratered regions on the scale of 1 – 100 km<sup>2</sup>. These wind directions are inferred from slip face orientations of intra-crater and inter-crater dunes. This study aims to better understand the correlation by quantifying the effects of crater topography on the near-surface wind regime. Digital Terrain Models (DTMs) from the High Resolution Imaging Science Experiment (HiRISE) are analyzed to determine the orientations and amplitudes of dunes in the equatorial region, and comparisons are made between similar geographic locations. Dune field orientation in Xainza Crater is shown to exhibit a 16.5° difference over a distance of ~2 km, and dune field orientations in Herschel Crater and Meroe Patera are shown to change by ~16° due to the presence of 500 – 1000 m diameter impact craters. Dune amplitude is not significantly affected by local topography. Crater topography thus introduces complexities to near-surface wind regimes that must be taken into account when comparing the results of local studies to GCMs and other theoretical models.

## Key Points:

1. Crater topography affects wind direction and dune field morphology in the equatorial region of Mars
2. Dune field orientations in Xainza Crater vary by 16.5° from crater center to crater rim
3. Impact craters with  $\leq$  1000 m diameter alter dune orientation by ~16° at 1 km distances

**Word Count:** 2195 words in text.

## 1 Introduction

Knowledge of global weather patterns provides insight into current climate conditions on Mars. When combined with an understanding of the planet's history, this information sheds light on the evolution of Martian climate and whether the planet may once have been habitable. Accurate weather models also help to determine the optimal locations for spacecraft landing sites. One of the most important components of a weather model is atmospheric circulation derived from global wind patterns. Aeolian (i.e. wind) processes cannot be directly measured, but they can be inferred from observations of their long-term effects on surface features and topography. On terrestrial planets such as Earth, the prevailing wind is capable of eroding sand and altering other environmental features. Sand dunes are among the most widespread aeolian features on Mars (Hayward et al., 2009). The formation of aeolian dunes requires a source of sand, sufficient wind strength to induce saltation and sand transport, and subsequent weakening of the winds to allow for grain deposition (Bagnold, 1941). Dune fields are thus created and shaped by prevailing wind patterns over a long period of time. The majority of Martian sand dunes are oriented transverse to the dominant wind and thus prove useful for determining direction of the near-surface wind regime (Liu & Zimbelman, 2015). Because dune fields on Mars are in equilibrium with current atmospheric conditions (Silvestro et al., 2010), slip face orientation measurements on dunes serve as truthful indicators of the prevailing near-surface wind. These patterns can be compiled and incorporated as parameters into wind models to contribute to a better understanding of present-day atmospheric conditions on Mars. Consequently, accuracy in the determination of local wind patterns is of paramount importance. The study of how crater topography affects local wind regimes is motivated by the observation that 78% of dune fields across all geographic locations on Mars are located within craters and ancient impact basins (Hayward et al., 2007).

Global Climate Models (GCMs) are used for weather forecasting, understanding the climate, and predicting climate change. The NASA Ames Research Center Mars GCM (Ames Mars GCM) is a mathematical model of circulation in the Martian atmosphere based on global parameters such as atmospheric density, atmospheric composition, and temperature. Apart from forecasting large-scale climate change, GCMs can also be used to predict local wind patterns — some on the scale of 5° latitude by 6° longitude — depending on the resolution of the model (McEwen et al., 2007). Previous scholars have noted that comparisons between Ames Mars GCM predictions and slip face orientations are inconsistent and often incompatible (Hayward et al., 2007), and that mesoscale (i.e. regional or topography-specific) wind models are more in agreement with local wind patterns determined by dune morphology in complex regions (Silvestro et al., 2010). Between 65°N and 65°S, for example, there is only a ~30% correlation between Ames Mars GCM wind directions

and dune slip face orientation for dune fields located within craters (Hayward et al., 2007). The percentage correlation between slip face orientations of inter-crater dunes and GCM winds in the equatorial region is approximately 50% but still reflects major differences between actual and modelled results (Hayward et al., 2009). The poor correlation between slip face measurements of intra-crater/inter-crater dunes and GCM-predicted winds motivates a study of the quantitative effect of crater topography on the near-surface wind regime.

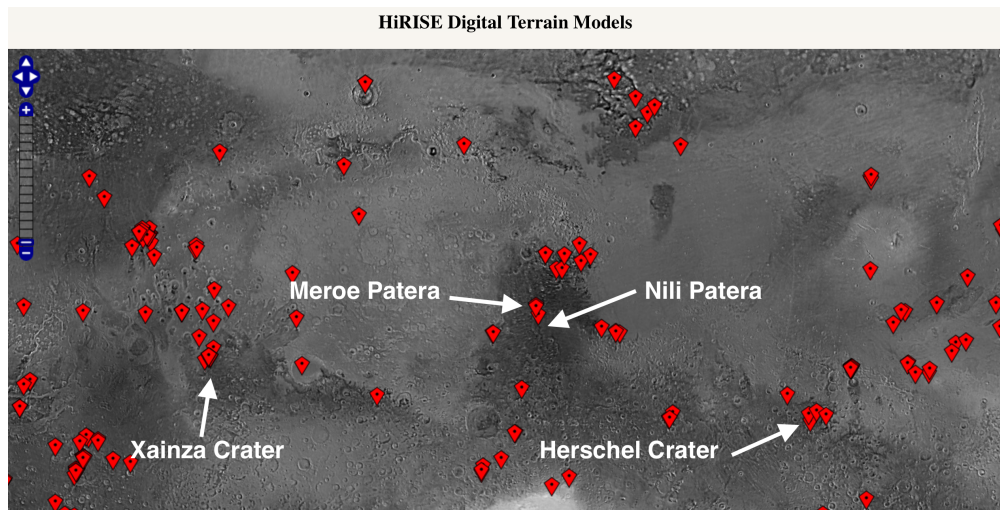


**Figure 1:** Two-dimensional projection of the equatorial region of Mars with approximate location of DTMs marked. The latitude in the image ranges from approximately 30°S at the bottom to 45°N at the top. The longitude spans 360° with the center of the image located at approximately 60°E.

Scholars have long recognized that stable topographic features such as craters and mountains possess the capability of influencing local wind strength and direction. These changes to the near-surface wind pattern then affect the development of unstable topographic features such as dune fields. Past studies of intra-crater dune fields in Gale Crater (Hobbs et al., 2010) and Proctor Crater (Fenton et al., 2005) have shown that there is a potential correlation between surface wind patterns, topographic setting, and, in turn, the characteristic dune morphology. Based on the presence of complex dunes and dune fields, Cardinale et al. (2012) conclude that the dune fields in Herschel Crater — in the Mare Tyrrenium Region — are affected by surface winds controlled by variable topography. A comprehensive study of Martian dunes initiated by Hayward et al. (2007) demonstrates that slip face orientations are not well-correlated with GCM output, suggesting that local topography has a significant influence on dune orientation. Hayward et al. (2007), on the other hand, focus on gross dune morphology in their analysis rather than individual slip face details. Gross dune morphology contributes to a global determination of wind direction and does not provide sufficient detail to infer local wind patterns. Furthermore, Hayward et al. (2007) only analyze

dunes formed under a unidirectional wind regime and do not address dune fields within craters whose morphology is governed by multiple converging winds.

This paper aims to address the lack of scholarship on how crater topography quantitatively affects the orientations and amplitudes of dunes located in the equatorial region of Mars. The study focuses primarily on dunes of the barchan and barchanoid variety (i.e. crescent-shaped and oriented perpendicular to the incoming wind) (Bagnold, 1941). Barchans and barchanoids are the dunes of choice because they accurately preserve the predominant wind direction. Other dune types, such as star dunes, preserve traces of multiple winds from different directions and do not offer conclusive evidence for a dominant wind pattern. Though the analysis is limited in terms of both geographic location and number of dune fields examined, it will serve as the first step towards a better and more detailed understanding of weather patterns on Mars.

## 2 Data and Methods

### HiRISE DTMs of Dune Fields in the Equatorial Region

Dune Location	Region	Latitude (°)	Longitude (°)
Xainza Crater	Meridiani Planum	-0.2	355.6
Herschel Crater	Mare Tyrrenium	-15.1	131.9
Herschel Crater	Mare Tyrrenium	-14.8	127.8
Nili Patera	Syrtis Major	8.8	67.3
Meroe Patera	Syrtis Major	7.2	67.8

Table 1: HiRISE DTMs

The six HiRISE DTMs selected for analysis. Refer to the Appendix (Section 7) for the original DTM images downloaded from <http://www.uahirise.org//dtm/>. Refer to Fig. 1 for a profile of the equatorial region of Mars and the approximate locations of the DTMs. The dune fields in Xainza Crater are located within a crater of diameter  $> 5$  km (Fig. 9). The barchan dunes within Herschel Crater appear modified by the presence of a smaller impact crater with diameter 500 m (Figs. 10 and 11). The presence of smaller craters affects average dune orientation and amplitude in the Nili Patera and Meroe Patera dune fields (Figs. 12 and 13).

All images are obtained from the Mars Reconnaissance Orbiter's (MRO) High Resolution Imaging Science Experiment (HiRISE) (Table 1). Refer to Fig. 1 for a reference map showing approximate locations of the images on the Martian surface. The images are formatted as DTMs that allow for determination of elevation differences and orientation relative to North. Applied geometric

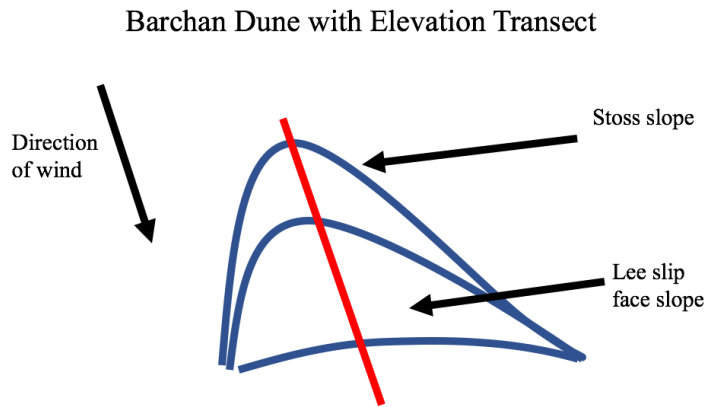


**Figure 2:** Diagram showing the method of dune field analysis. The shape in blue is the top view of a typically shaped barchan dune. The red line is an elevation transect.

corrections lead to topographic measurements with better than 25 cm vertical precision (McEwen et al., 2007).

The study narrows its focus on barchan and barchanoid dunes to facilitate comparisons across different regions. Barchans and barchanoids are also among the most relevant dune types to analyze because 63% of dune fields in the equatorial region are composed of one or the other (Gardin et al., 2011). The five study sites chosen all lie within  $15^{\circ}$  of the equator and are not clustered longitudinally (Table 1). The two dune field features analyzed are dune orientation and dune amplitude. These two characteristics are simple to measure and can be accurately determined from the DTMs. Furthermore, they reveal the most information about the local wind regime because dune orientation is directly related to wind direction, while dune amplitude strongly correlates with wind strength (Bagnold, 1941).

The first region of interest is Xainza Crater ( $-0.2^{\circ}$ ,  $355.6^{\circ}$ ) in the Meridiani Region. The two distinct dune fields lie at different distances from the crater center and thus likely exhibit different characteristic orientations and dune amplitudes (Fig. 9). The second site is Herschel Crater ( $14.8^{\circ}$ ,  $127.8^{\circ}$ ), a 300-km-diameter impact basin situated in the cratered southern highland in the Mare Tyrrenium Region (Cardinale et al., 2012). The presence of smaller impact craters motivates study of Herschel Crater dune fields to determine the effects on wind orientation from local topography (Figs. 10 and 11). A third site is Nili Patera ( $8.8^{\circ}$ ,  $67.3^{\circ}$ ) in the Syrtis Major Region, where the observed dunes show signs of recent activity (Gardin et al., 2011). The dunes at Meroe Patera ( $7.2^{\circ}$ ,  $67.8^{\circ}$ ) — also in the Syrtis Major Region — are in close proximity and motivate comparison of dune amplitudes and orientations with Nili Patera.

Slip face measurements are made from elevation transects that begin on the upwind stoss slope and end on the lee slip face slope of a dune (Fig. 2). The lines are parallel to the direction of sediment transport and therefore indicative of the overall direction of the prevailing wind (Liu & Zimbelman, 2015). The orientation of the line relative to North indicates the orientation of the dune, and the amplitude of the dune is determined from finding the maximum elevation along the line. Eight elevation transects are sampled for each of eight barchan dunes in the regions of study. Amplitudes and orientations calculated from each line are collected into histograms for analysis and comparison between regions.

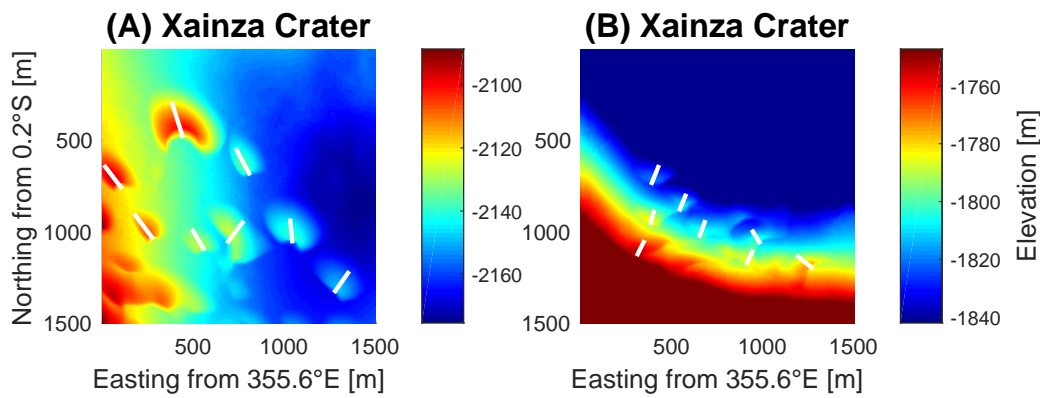


**Figure 3:** Cropped and thresholded DTM of dunes in Xainza Crater. Refer to the Appendix (Section 7) Fig. 9 for a map of the entire region. (A) Dune field located at crater center. White lines represent elevation transects over barchan dunes. (B) Dune field located 2 km southwest of crater center.

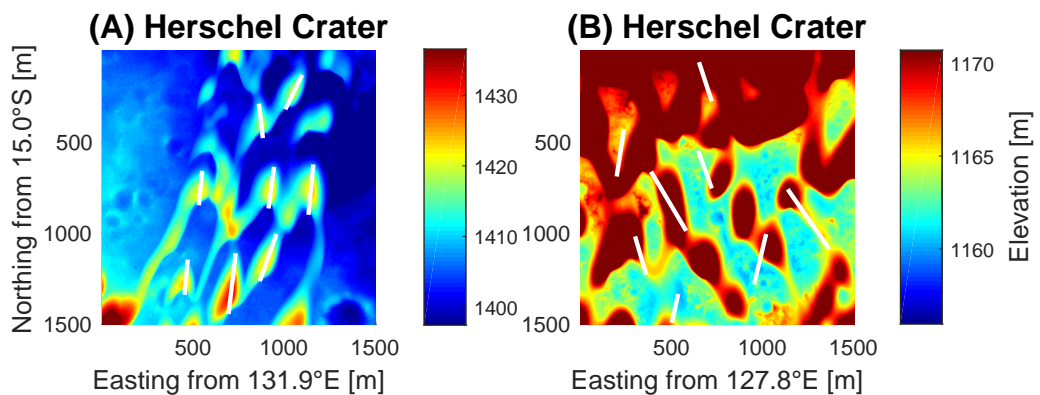


**Figure 4:** (A) Cropped and thresholded DTM of Herschel Crater dunes. White lines represent elevation transects mapped onto barchan dunes. (B) Cropped and thresholded DTM of dark dunes in Herschel Crater. Refer to Figs. 10 and 11 for full-scale maps.

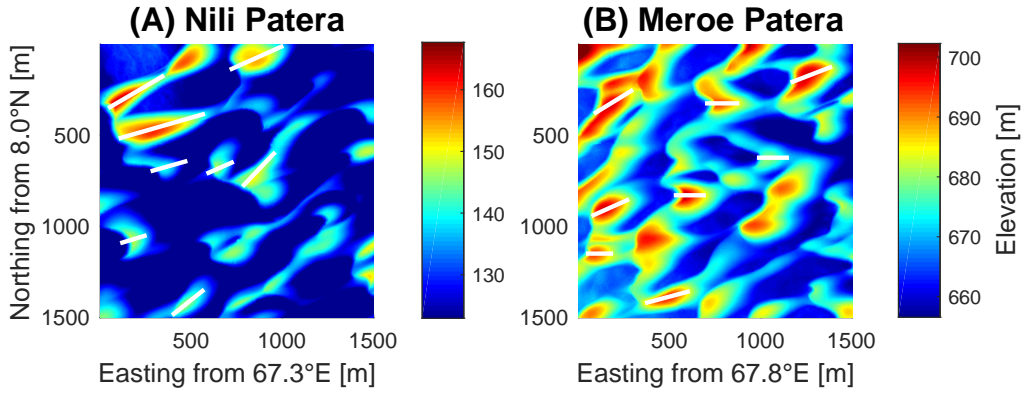


**Figure 5:** (A) Cropped and thresholded DTM of dunes in Nili Patera. (B) Cropped and thresholded DTM of dunes situated west of Meroe Patera. Refer to Figs. 12 and 13 for full-scale maps.

### 3 Results

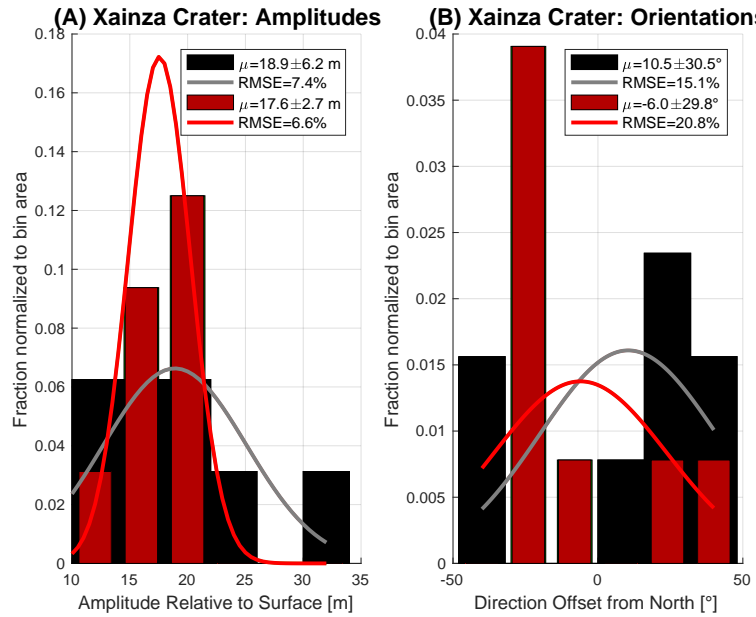


**Figure 6:** (A) Histogram of dune amplitudes of two separate dune fields located in Xainza Crater (Fig. 3). The barchan dunes at the center of the crater (black) have amplitudes mostly in the range of 10 – 25 m; the barchan dunes near the southwest crater rim (red) are all in the range of 10 – 20 m. (B) Dune orientations are not clustered and show high variability. The barchan dunes located at crater center (black) have an average angle of  $10.5^\circ$  clockwise from North, whereas the dunes southwest (red) have an average angle  $6.0^\circ$  counterclockwise from North.

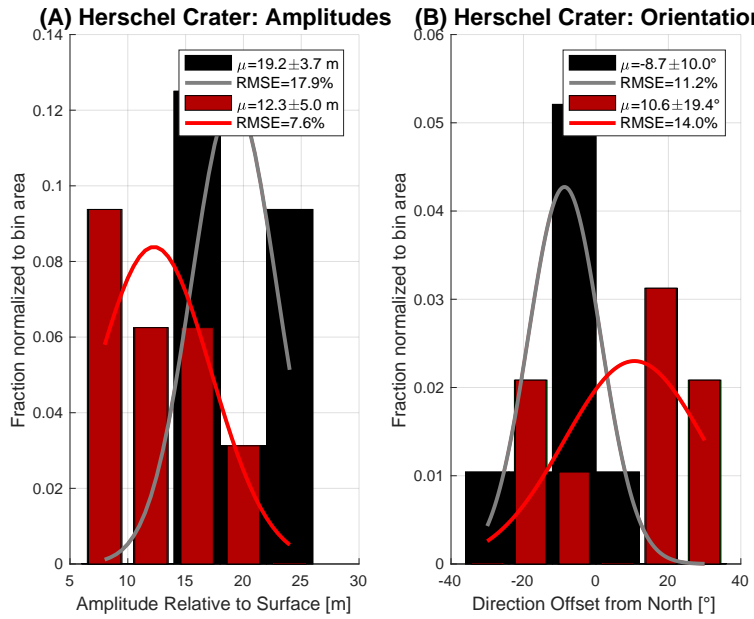


**Figure 7:** (A) Histogram of dune amplitudes of two dune fields in Herschel Crater. The black bars indicate dunes located  $\sim 1$  km away from a 500 m diameter impact crater. Dune amplitude values for both fields are clustered, but there is a 5.8 m difference in mean amplitude between dunes close to the crater and dunes much further away. (B) Orientations relative to North show high variability. The dunes close to the impact crater have an average angle of  $8.7^\circ$  counterclockwise from North. The dunes far away are on average  $10.6^\circ$  clockwise from North.

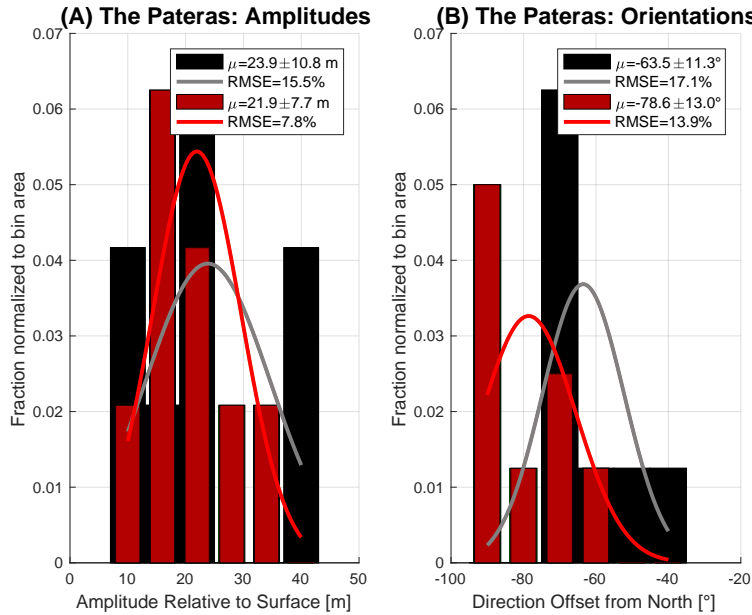


**Figure 8:** (A) Histogram of barchan amplitudes of dune fields in Nili Patera and Meroe Patera. The dunes in Meroe Patera are situated  $\sim 1$  km away from a 1 km impact crater, but both dune fields are clustered and their average amplitudes are within 2.0 m of each other. (B) Similar to Figs. 6 and 7, dune orientations are variable and correlate poorly with a normal distribution. The two dune fields differ in average angle offset from North by  $15.1^\circ$ .

## 4 Discussion

Fig. 6 shows that dune amplitudes in the two fields in Xainza Crater are clustered around an average value of  $\sim 18.0$  m. The high degree of clustering is evidence of a prevailing wind characterized by steady velocity. However, the dune orientations do not center on an average value and instead are scattered with standard deviation of  $\sim 30.0^\circ$  on either side of North. The dunes located near the southwest crater rim have an average orientation that differs from the dunes at center by  $16.5^\circ$ . The significant variation in angle indicates an inconsistent wind pattern and suggests that the crater wall plays a role in shaping local wind direction.

In their study of Herschel Crater, Cardinale et al. (2012) demonstrate that the orientation of slip faces in intra-crater dune fields is strongly topographically controlled. Dune fields located around 23-km-diameter and 45-km-diameter craters exhibit slip face orientations characterized by high values of standard deviation and thus high dispersion, whereas dune fields outside these craters exhibit more clustered values of slip face orientation that are in agreement with GCM-predicted wind directions (Cardinale et al., 2012). Results from Fig. 7 support their claim since the standard deviation values for orientation of dunes close to a small impact crater and dunes far away are  $10.0^\circ$  and  $19.4^\circ$ , respectively. Moreover, unlike the amplitudes of dune fields in Fig. 6, Herschel Crater dune amplitudes are clustered but differ in mean value of 5.8 m. The inconsistency may be a result of varying wind speeds at the two locations or too narrow a sample of barchan dunes. Further investigation is required to resolve this difference. Cardinale et al. (2012) further determine that the dunes in Herschel Crater were accumulated by a prevailing wind from the North, and that the wind direction subsequently was modified by local crater topography. This is in agreement with calculated dune orientations as the averages ( $-8.7^\circ$  and  $10.6^\circ$ ) are relatively close to zero when considering the full  $360^\circ$  range available (Fig. 7).

Similar to the dune fields in Xainza Crater, Fig. 8 shows that dune amplitudes in Nili Patera and Meroe Patera also approximately fit a normal distribution and cluster around a common average value. The dune fields were thus shaped by winds with relatively constant strength. Unlike the results calculated in Figs. 6 and 7, however, slip face orientations for the Pateras regions reveal significant clustering and little variability as demonstrated by low standard deviation values compared to the average. From observations of both wind streaks and dune morphology, Gardin et al. (2011) infer a dominant wind direction coming from the north in the Nili Patera region, but this is not entirely correct. Elevation transect analysis instead shows a dominant wind from the northeast.

Hayward et al. (2014) show that between  $40^\circ\text{S}$  and  $70^\circ\text{N}$ , wind directions derived from slip face measurements are evenly distributed and do not exhibit a predominant direction. The combined

results affirm this claim because the dominant wind direction in the Xainza Crater and Herschel Crater regions is north to south, whereas the dominant wind direction in the Pateras is oriented northeast to southwest.

## 5 Conclusions

Dune field orientation in Xainza Crater is shown to exhibit a  $16.5^\circ$  difference over a distance of  $\sim 2$  km from crater center, and dune field orientations in Herschel Crater and Meroe Patera are shown to change by  $\sim 16^\circ$  due to the presence of 500 – 1000 m diameter impact craters. Dune amplitudes are not significantly affected by local topographic effects as values exhibit a high degree of clustering. These first results are an attempt to quantify the significant effect of crater topography on the near-surface wind regime. Further mapping of intra-crater and inter-crater dune fields — not only in the equatorial region but also the north and south pole regions — could lead to potential models of topographical effects that could then be factored into GCMs for a more accurate determination of Martian weather and climate. A more nuanced understanding of the red planet serves space agencies and climate scientists equally well and even further contributes to insight of Earth's own climatic history.

## 6 Acknowledgements

I would like to thank Adam and Frederik for teaching me about dune morphology, providing me with template code and analysis ideas, and giving me the confidence — through their inspiring instruction — to conduct my own investigations. I would like to thank my classmates in FRS124 for serving as an audience to whom I could pitch and test my proposals and thoughts.

## 7 Appendix

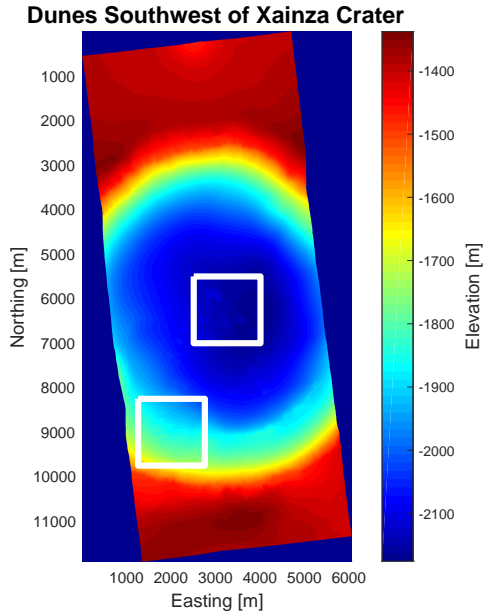


**Figure 9:** HiRISE DTM of Dunes and Slopes Southwest of Xainza Crater. The areas of interest in the image are outlined by white rectangles. Both 1500 m-by-1500 m regions contain barchan dune fields with characteristic orientation and amplitude.

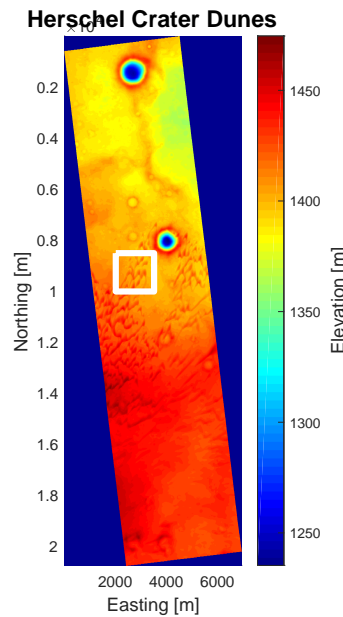


**Figure 10:** HiRISE DTM of Herschel Crater Dune Changes. The outlined area of interest lies approximately 1 km to the southwest of the small impact crater.

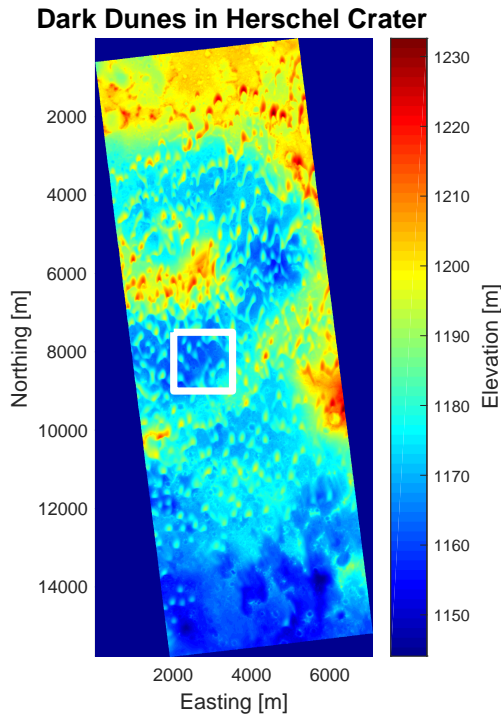


**Figure 11:** HiRISE DTM of Dark Dunes in Herschel Crater. A typical example of barchan dunes formed within a large crater basin. The white rectangle denotes the regions chosen to be representative of the entire dune field.

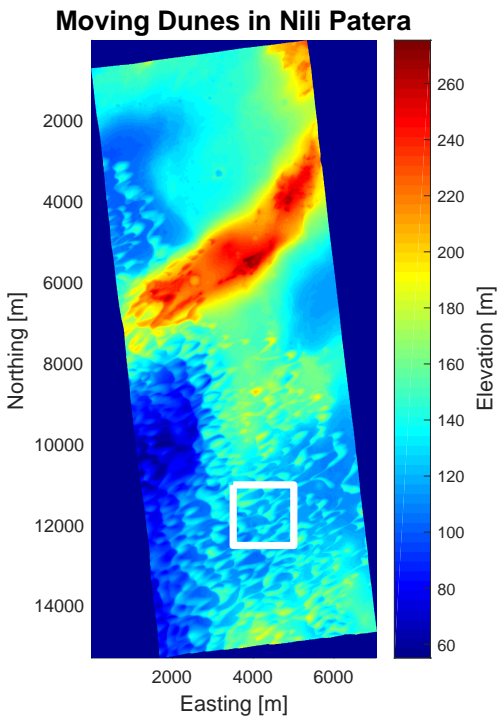


**Figure 12:** HiRISE DTM of Moving Dunes in Nili Patera. Dark dunes in the region of study display signs of recent activity.

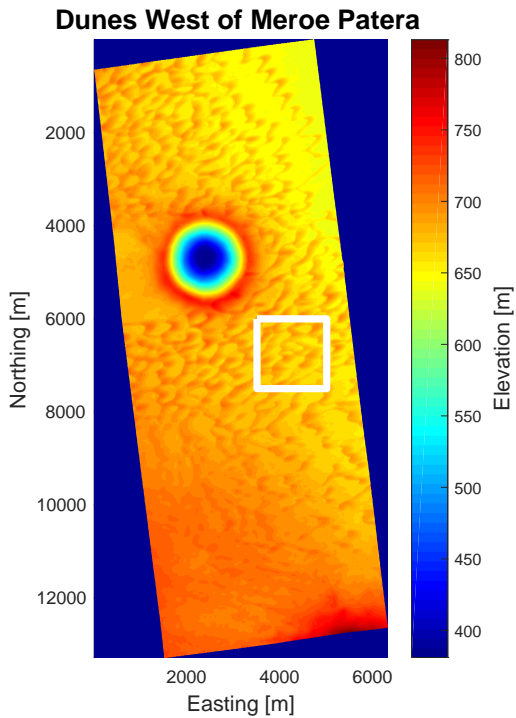


**Figure 13:** HiRISE DTM of Dunes West of Meroe Patera. The outlined area of interest lying to the southeast is at a radial distance of 1 km from the center of the small impact crater.

## References

- Bagnold, R. A., 1941. *The Physics of Blown Sand and Desert Dunes*, Methuen, London.
- Cardinale, M., Komatsu, G., Silvestro, S. & Tirsch, D., 2012. The influence of local topography for wind directions on Mars: two examples of dune fields in crater basins, *Earth Surf. Process. Landforms*, **37**(13), 1437–1443.
- Fenton, L. K., Toigo, A. D. & Richardson, M. I., 2005. Aeolian processes in Proctor Crater on Mars: Mesoscale modeling of dune-forming winds, *J. Geophys. Res.*, **110**(E6), 1–18.
- Gardin, E., Allemand, P., Quantin, C., Silvestro, S. & Delacourt, C., 2011. Dune fields on Mars: Recorders of a climate change?, *Planetary and Space Science*, **60**, 314–321.
- Hayward, R. K., Mullins, K. F., Fenton, L. K., Hare, T. M., Titus, T. N., Bourke, M. C., Colaprete, A. & Christensen, P. R., 2007. Mars Global Digital Dune Database and initial science results, *J. Geophys. Res.*, **112**(E11), 1–17.
- Hayward, R. K., Titus, T. N., Michaels, T. I., Fenton, L. K., Colaprete, A. & Christensen, P. R., 2009. Aeolian dunes as ground truth for atmospheric modeling on Mars, *J. Geophys. Res.*, **114**(E11), 1–11.
- Hayward, R. K., Fenton, L. K. & Titus, T. N., 2014. Mars Global Digital Dune Database (MGD3): Global dune distribution and wind pattern observations, *Icarus*, **230**, 38–46.
- Hobbs, S. W., Pauli, D. J. & Bourke, M. C., 2010. Aeolian processes and dune morphology in Gale Crater, *Icarus*, **210**(1), 102–115.
- Liu, Z. Y.-C. & Zimbelman, J. R., 2015. Recent near-surface wind directions inferred from mapping sand ripples on Martian dunes, *Icarus*, **261**, 169–181.
- McEwen, A. S., Eliason, E. M., Bergstrom, J. W., Bridges, N. T., Hansen, C. J., Delamere, W. A., Grant, J. A., Gulick, V. C., Herkenhoff, K. E., Keszthelyi, L., Kirk, R. L., Mellon, M. T., Squyres, S. W., Thomas, N. & Weitz, C. M., 2007. Mars Reconnaissance Orbiter's High Resolution Imaging Science Experiment (HiRISE), *J. Geophys. Res.*, **112**(E5), 1–40.
- Silvestro, S., Fenton, L. K., Vaz, D. A., Bridges, N. T. & Ori, G. G., 2010. Ripple migration and dune activity on Mars: Evidence for dynamic wind processes, *Geophys. Res. Lett.*, **37**(20), 1–6.